A new model for droplet – solid surface interaction. Impingement onto hydrophilic and superhydrophobic surfaces

I. Malgarinos[1,*], M. Marengo[2], C. Antonini[3], N. Nikolopoulos [1], G. Strotos[1], and M. Gavaises[1]

1: School of Engineering and Mathematical Sciences, City University London, Northampton Square, EC1V 0HB London, UK, *Corresp. Author – e-mail: Ilias.Malgarinos.1@city.ac.uk
2: Department of Engineering, University of Bergamo, viale Marconi 5, 24044 Dalmine, Italy
3: Laboratory of Thermodynamics in Emerging Technologies, Mechanical and Process Engineering Department, ETH Zurich , Sonneggstrasse 3, 8092 Zurich, Switzerland

Abstract

In this study, a new model for the wetting interaction between a liquid droplet and a solid surface is presented. Based on this model, a force which acts on the contact line is incorporated as a source term in the Navier-Stokes momentum equation. The advantage of the new model in comparison with the widely-used Brackbill's model is that the contact angle is not inserted as a boundary condition, but is derived by the induced fluid flow and the adhesion physics of the liquid-surface combination. For the interface tracking, the Volume of Fluid (V.O.F) method is used, accompanied by an automatic local grid refinement technique in order to minimize the arithmetic diffusion of volume fraction and thus acquire more representative physical results. The new model is validated against experimental data for low and moderate We numbers both for hydrophilic and superhydrophobic surfaces. Results of the model are also compared against the standard Brackbill's model for the implementation of the wetting force. The apparent contact angle during droplet spreading and recoiling is plotted in order to gain insight on the dynamic angle temporal evolution during the impingement process.

Introduction

Droplet impingement is an area of fluid mechanics that concerns a vast number of technological applications varying from spray cooling and spray coating to combustion in internal combustion engines. Most recently, hydrophobic and super-hydrophobic surfaces have attracted the interest of many researchers due to their ability to repel water droplets, which in turn gives them the most significant advantage, among other surfaces, of self-cleaning (like lotus leaves). Many researchers have fabricated new materials using different ways (chemically, or mechanically treated surfaces) with varying surface roughness that show different behavior in terms of their interaction with liquid droplets [1]. The main focus of researcher's interest is to predict either qualitatively or quantitatively the interaction of liquid droplets with a solid surface, and finally achieve to control the contact time of the droplet onto this surface. In this way, the main advantages of large contact times can be exploited in cases of spray cooling for example, while for surfaces, which need to be self-cleaned, (as airfoils – avoid solidification, or photovoltaic panels) the minimum contact time is requested to be achieved.

So far, a vast number of experimental studies [2-6] have focused on the temporal evolution of a droplet spreading on a solid substrate in relation to the droplet's properties (surface tension, impact velocity, initial radius), as well as the properties of the solid surface (wettability, roughness). Most recently, due to the great advancements in photography, researchers can focus on more microscopic details of the process, such as the dynamic contact angle and the velocity of the rim throughout the evolution of the phenomenon [6-8]. Based on these experiments, it is proved that the contact angle between the droplet and the solid surface changes throughout the advancing and receding phases of droplet spreading. In order to account for this change, many dynamic contact angle models concerning CFD simulations can be found in literature, a review of which is given in [9]. However, as Yokoi et al. [10] suggest, the change in contact angle values which are implemented in a CFD simulation can affect the outcome of the impingement process. In all cases mentioned, the contact angle is not derived based on the induced flow, but is implemented in the momentum equation as a boundary condition. Therefore, a new model needs to be developed that can dynamically alter the contact angle based on the fluid flow and operating conditions, rather than insert it as a boundary condition.

Mathematical modelling

For solving the two-phase flow of a liquid droplet impinging on a flat surface, the Volume of Fluid Method (V.O.F) [11] is used, using the CSF model for the surface tension force term in the momentum equation (see Brackbill et al. [12]). The solution of V.O.F equations is executed in ANSYS FLUENT solver, where the axi-symmetric approach is adopted (along the mass centre of the droplet) for minimization of the computational cost. In order to keep the interface as sharp as possible and avoid numerical diffusion, an automatic adaptive grid refinement technique is used, similar to the one proposed by Theodorakakos et al [13]. This method has been successfully applied by Nikolopoulos et al. [14], Strotos et al. [15, 16] in cases concerning droplet impingement, collision and splashing onto a liquid film, with and/or without heat transfer, making it a reliable way to save computational time and retain a fine level of accuracy. The model for adaptive local grid refinement was implemented in ANSYS/FLUENT commercial software via User Defined Function (UDF). For the discretization of the advection term in the volume fraction equation, the high-resolution HRIC scheme [17] is used. At the end of every time-step, an additional equation, which was proposed by Olsson et al. [18] and used in Level-Set, is solved in order to keep interface thickness constant to approximately 3 cells. This equation is:

$$\frac{\partial \alpha}{\partial \tau} + \beta \nabla \cdot \alpha(1-\alpha) = \beta \varepsilon \nabla \cdot (\nabla \alpha) \tag{8}$$

Equation (8) is solved once (for one $\Delta\tau$) in pseudo-time with time-step equal to the advection time-step, while ε takes the value of $\Delta x/2$ (where Δx is the grid cell edge, as proposed in [19]). The additional variable β is proposed by Sato et al. [19] in order to avoid deformation in droplet shape and it is reported to take values in the range from 0.01 to 1. In this study, β is set equal to 0.25 throughout the domain, which by a number of numerical tests undertaken, is proven to be both compressive, as well as enough for the mass conservation of the volume fraction field. Pressure – Velocity coupling is achieved by adopting a coupled approach [20], for which momentum and pressure-based continuity equations are solved together, while the Rhie-Chow pressure dissipation terms are included in the face mass fluxes. The time-step of the calculations, is varying for all simulations, so that the Courant number can be kept constant at around 0.25. The solution of equation (8) was implemented in FLUENT through a user-defined scalar, while its solution was implemented via UDFs.

Wetting Force

The wetting angle of the droplet with the solid surface is a matter of great interest. The interaction between liquid and solid surface molecules in the three-phase contact line of the drop is what determines microscopically the angle which is formed, and macroscopically the maximum spread of the droplet, as well the contact time on the surface, which are the main areas of interest that concern industrial applications. So far, the most widely-used model in VOF, for the implementation of the wetting angle, is the approximation proposed by Brackbill et al. [12]. In this paper, a new model is proposed for contact angle implementation, in which contact angle is derived from the induced fluid flow. Based on this model, it is assumed that a force acts on the contact line, as proposed in [21]. If energy is assumed to be conserved in the 3-phase contact line, as proposed by Young, for a static droplet, then the force acting on the rim is tangent to the liquid-gas interface (Figures 1a,b).

In relation to the typical friction force, the adhesion force, is assumed to be higher when the droplet is static and is lower when the droplet is moving (in case of sliding, for example Figure 1a). As the contact line moves (Figure 1b), its value is equal to:

$$\begin{aligned} f_{\sigma mar} &= \sigma\left[\cos(\theta_{eq}) - \cos(\theta_{app})\right] r \quad \text{if } v_{conline} > 0 \text{ or } v_{conline} < 0 \\ f_{\sigma mar} &= \sigma\left[\cos(\theta_{eq})\right] r \qquad\qquad\qquad \text{if } v_{conline} = 0 \end{aligned} \quad \text{[N]} \tag{9}$$

where:

$$\begin{cases} \theta_{eq} = \theta_{adv} & \text{if } v_{conline} \geq 0 \\ \theta_{eq} = \theta_{rec} & \text{if } v_{conline} < 0 \end{cases} \tag{10}$$

θ_{adv} and θ_{rec} are the advancing and receding contact angle, respectively, measured using the standard sessile drop method, i.e. while expanding and retracting a drop quasi-statically on a horizontal surface; their difference, $\Delta\theta = \theta_{adv} - \theta_{rec}$, is the contact angle hysteresis. During the spreading/receding phase, if the apparent contact angle is higher than the equilibrium, the force would be positive, trying to accelerate the rim and reach θ_{eq}., while if it is lower, then the force would take negative value. This force is higher for large differences between the equilibrium and the apparent contact angle. For the time instant when the velocity of the contact line approaches zero, the value of the force is higher, and results in the deformation of the rim, so that it can reach its receding shape beginning from its advancing one. This "contact line stress" (equation 9) is incorporated in the momentum

equation as a source term only on the interface-contact line cells, namely the boundary wall cells where volume fraction is neither 0 nor 1. As for the model expression (equation 9), the part which concerns the force when the rim velocity is equal to zero (mainly during the "hysteresis" time), was not used in the scope of the present study due to the high uncertainty to define the time instant when $v_{conline} = 0$. For the remainder of this paper, the wetting force model will be referred as Marengo's Force Model.

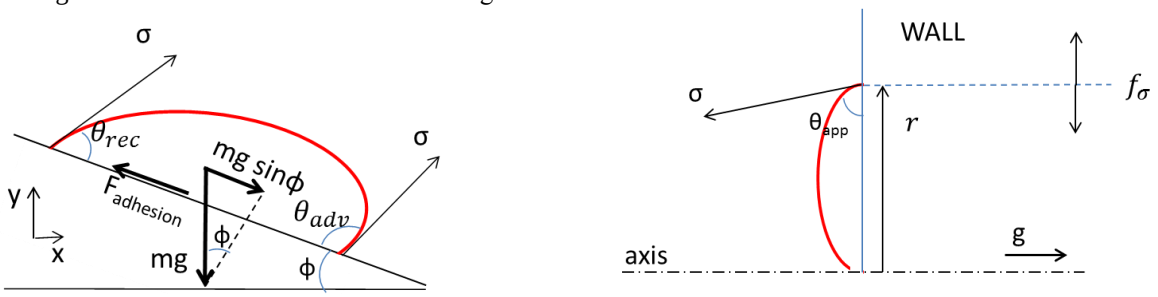

(a) (b)

Figure 1. (a) Adhesion force for a liquid droplet sliding down an incline, (b) Direction of the wetting force (Marengo's Force Model) on a typical time instant of a droplet spreading on a wall (axisymmetric case)

An advantage of using this approach instead of the typical Brackbill's model would be the dynamic tracking of the apparent contact angle, which could shed light in the impinging process from the contact angle viewpoint.

Four cases are used for the validation of the new model, which are summarized in Table1 and concern the impingement of a water droplet on a hydrophilic and a Super-Hydrophobic surface, at low and moderate We numbers. For the numerical validation of the new methodology, results of the Marengo's Force Model are compared against the ones derived using the Brackbill's approach.

	R_0(mm)	We	θ_{adv}	θ_{rec}	ξ_{max} Exper	ξ_{max} Theoret [22]	ξ_{max} Brackbill	ξ_{max} Marengo's Force Model	Reference
Case1	1.43	30	48	5	2.60	3.51	3.61	3.55	[2]
Case2	1.43	92	48	5	3.60	3.98	4.20	4.16	[2]
Case3	1.43	29	162	154	1.75	2.24	1.81	1.72	[2]
Case4	1.43	93	162	154	3.06	3.02	2.52	2.58	[2]

Table1. Test cases used for the validation of the methodology.

Results and Discussion

In Figure2, the dimensionless maximum droplet spreading radius is plotted against We number for the four cases listed in Table1, as it is derived from the two models described above (Brackbill, Marengo's Force Model) together with the experimental values gathered from the work of Antonini et al. [2]. In this Figure, it is deemed necessary to include the maximum droplet spreading as it results based on the theoretical equation of Pasandideh-et al. [22]:

$$\frac{D_{max}}{D_0} = \sqrt{\frac{We + 12}{3(1-\cos\theta) + 4(We/\sqrt{\mathrm{Re}})}} \quad (12)$$

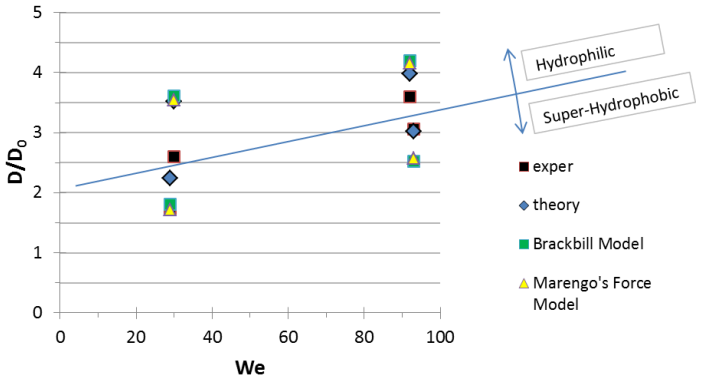

Figure 2. Comparison of dimensionless maximum spreading (D/D_0), predicted by the different numerical models and the experimental data.

because of the overprediction of droplet spreading from the simulation. This equation has resulted from the energy balance of kinetic and surface energy, before impact and at maximum spreading, where the work loss due to viscous dissipation is accounted for, while the droplet is assumed to take the shape of a cylinder with height as much as its splat thickness at maximum spreading. Results of the simulation are much closer to this equation, as expected, due to the fact that the exact experimental conditions (e.g. oscillations of the droplet just before its impact) or crucial operating conditions such as surface roughness cannot be included in the CFD model. Therefore, simulation results can be compared with better certainty with these theoretical values. However, the

comparison between the experimental values together with the theoretical and the simulation results can give insights as to what can be missing based on the aforementioned assumptions.

Low We number

For the super-hydrophobic surface, results for both models (Brackbill – Marengo's Force Model) seem to be in very good agreement with the experimental values as well as with the theoretical ξmax from equation (12). This means that the force that is assumed to act on the rim is very close to the one which appeared during the experiment. As for the hydrophilic glass surface, maximum spreading is highly overestimated, when it is compared to the experimental data. However, it is much closer to the theoretical ξ_{max}, given by Pasandideh's simple equation. As this equation results from a simple energy conservation, and this theoretical value is in very good accordance with the results of the simulation, this means that the net force, assumed to exert on the rim, is not enough for the CFD simulations to reach the experimentally measured maximum spreading. Therefore, it is believed, that an adhesion force, counteracting the free movement of the droplet onto the solid surface as it spreads on it, is believed to be missing from the implementation of the momentum equation near the boundary cells. To sum up, for low We number, where the effect of inertia in relation to surface tension is small, two different behaviors are observed. For a hydrophilic surface, where small values of contact angle are apparent, a significant over prediction of maximum spreading is observed, while in comparison to the case of a hydrophobic surface the results are more promising. This disagreement between the numerical simulations and the experimental data may be as well attributed to experimental uncertainties in terms of contact angle measurement, which are of high importance for the validation and the right implementation of a numerical model, in all cases.

Moderate We number

Turning now to the cases with moderate We number, different behaviours are observed. For hydrophilic surfaces the maximum spread is again overestimated, however the deviation is lower than the corresponding one of the low We number impact. On the other hand, for the superhydrophobic surface, the increase of the We number resulted in the further underestimation of maximum spreading. This means that by increasing the effect of inertia while keeping surface tension effects constant, the net force that is applied on the rim in the CFD simulation is closer to the experiment for the hydrophilic surface than that for the hydrophobic surface. This, in turn, means that inertia plays an important role to the evolution of the phenomenon, and that the wetting forces exerted in real life (as well as the experiment) change according to the initial kinetic energy and impingement conditions. For a hydrophilic surface and for a low We number impact, stronger forces, than the one predicted by the numerical models, dominate. As the We number is increasing, these forces become more insignificant. For a hydrophobic surface, on the other hand, it seems that as the We number increases the wetting forces of the simulation are much stronger than the ones the experiment suggest, implying that the forces that act on the rim are more significant in the case of a superhydrophobic surface than the hydrophilic one. However, again uncertainties in terms of contact angle measurements are of importance. Figures 3 and 4 depict the temporal evolution of the dimensionless spreading radius, as a function of the maximum spreading value, D_{max}.

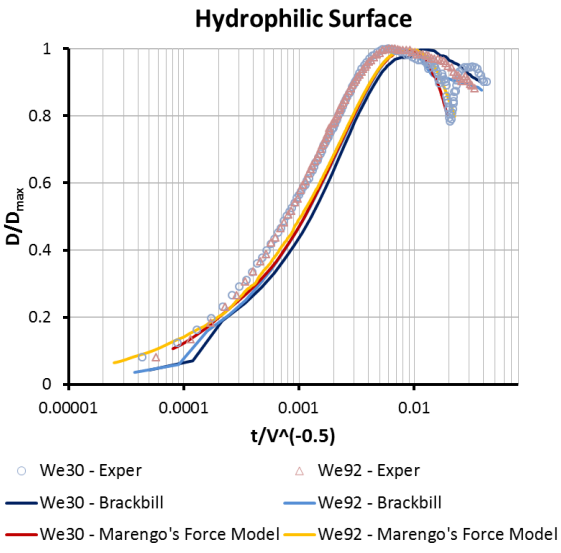

Figure 3. Comparison of the time that droplet reaches its maximum radius for Brackbill's Model, Marengo's Force Model and experiment. X axis is logarithmic.

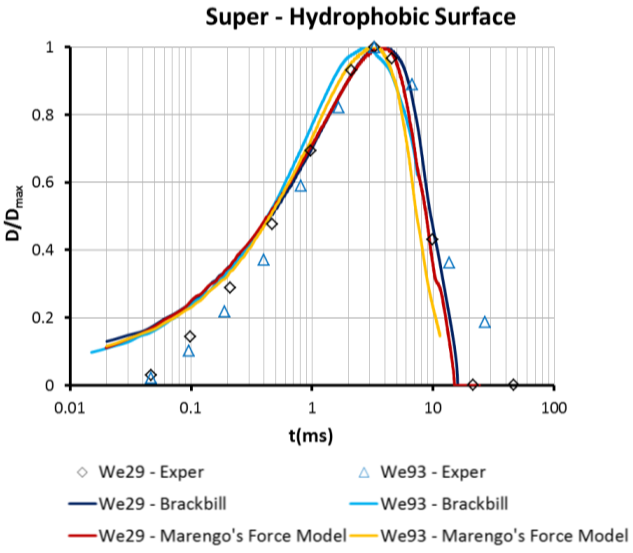

Figure 4. Comparison of the time that droplet reaches its maximum radius for Brackbill's Model, Marengo's Force Model and experiment. X axis is logarithmic.

The numerical results after the implementation of both models against the measured values are given. For the hydrophilic surface, time is divided by $U_0^{-0.5}$, in accordance with the work of Antonini et al. [2], who suggest that for a hydrophilic surface, the time that a droplet reaches its maximum radius, is constant, if divided by this value. This is obvious for the simulation results too. It is also clear that although in the case of We = 30, where maximum spread is greatly overestimated, its time derivative, until this maximum is reached is much closer to the experiment, showing that the simulation results agree qualitatively very well with the experiment. For both cases, however, this characteristic time, as predicted, is a little higher than the one measured, suggesting that this adhesion-like force should exist. For the hydrophobic surfaces, the actual time of the impingement is plotted, while the numerical results are in good agreement with the experimental values, depicting again that although maximum spread from the simulation may deviate from the experiment, the temporal evolution of the phenomenon is described accurately enough.

Effect of adhesion force

The implementation of the new model (Marengo's Force Model) does not seem to affect the macroscopic results (maximum spreading) of all four cases examined, when compared to the Brackbill's model. Nevertheless, the Marengo's Force Model, during the receding phase of the droplet impacting onto the hydrophilic surface, induces a smaller hysteresis time and thus faster receding phase. This is clearly shown in Figure 5, where the slope for the receding phase is much steeper.

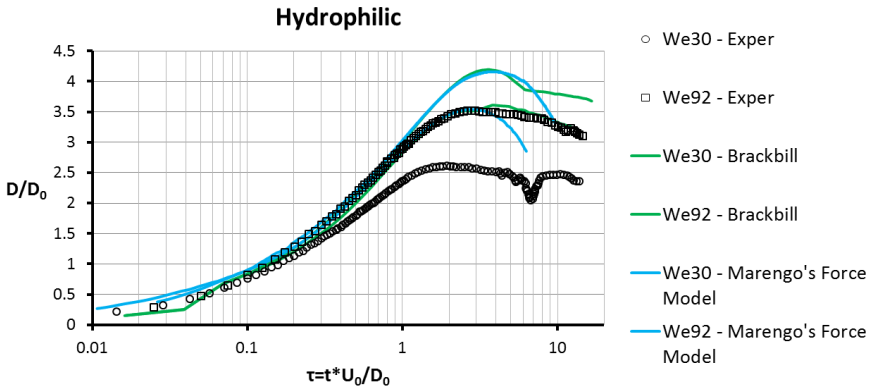

Figure 5. Dimensionless spread factor plotted against dimensionless time for a hydrophillic surface.

For the super-hydrophobic surface, although the maximum spreading results are similar for both models, the temporal evolution of the phenomenon is predicted more accurately by the Marengo's Force Model, as depicted in Figure 6. As discussed above, for the superhydrophobic surface, for low We numbers, where the effect of inertia is smaller, the Marengo's Force Model predicts more accurately the wetting effects during the impingement process. Further increase of the We number, results in a significant divergence between the experimental data and the simulation results, despite the fact that the trend of the line is similar to the one measured, showing that at least qualitatively, the temporal evolution of the impingement process is accurately described.

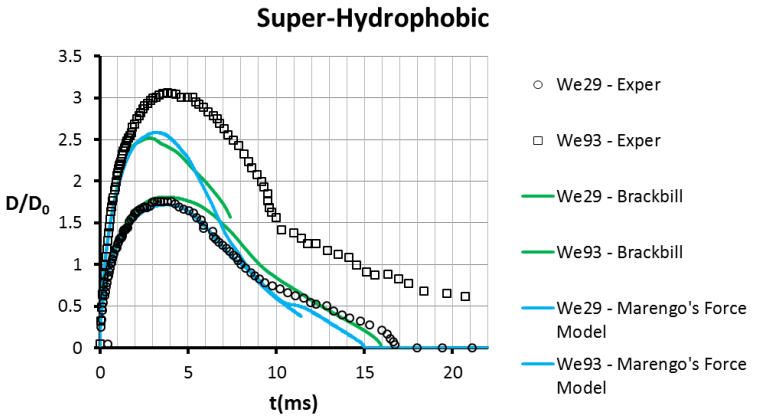

Figure 6. Dimensionless spread factor plotted against real time (in ms) for a superhydrophobic surface.

Figure 7 shows the temporal evolution of the impingement process for Case3. The similarities between the two models are obvious. Marengo's Force Model predicts a quicker receding phase, which is closer to the experiments. Furthermore, the angle which is observed for both the advancing and receding phases is bigger for Marengo's Model.

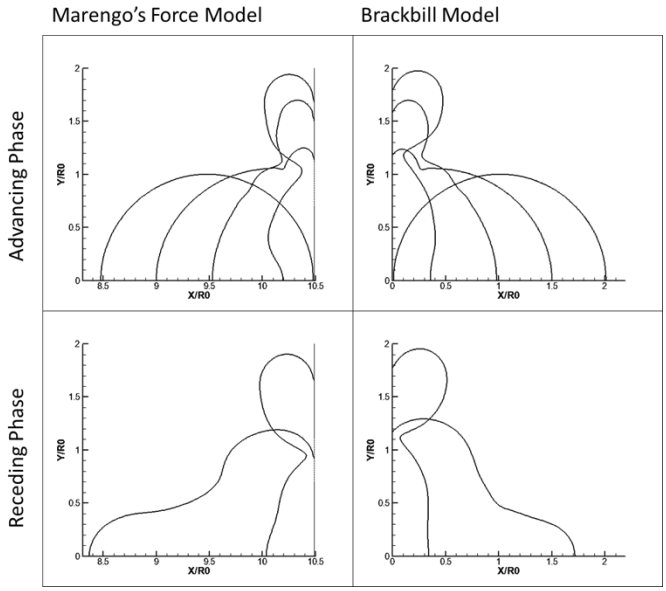

Figure 7. Temporal evolution of the impingement process for Case 3 of Table1. Results of the isoline of VOF = 0.5 are depicted for t=0, 0.9, 1.9, 3.9ms (advancing phase), and t=4.7, 8.4ms (receding phase).

Finally, Figure 8 depicts the temporal evolution of the apparent contact angle for Case 3 (We = 29 - impingement on superhydrophobic surface), which is a novel information, not previously presented in CFD calculations. This information is of high added value for the further validation of the model as well as for the experiments to comment on in future works. From this Figure, it is clear that the apparent contact angle increases during the first stage of impingement, then it remains approximately constant at around 155 degrees, while during the receding phase it reduces rapidly to 145 and then fluctuates around this value. The noise in the graph can be attributed to the choice of the contact line cell, where this velocity is measured. For the scope of this study, the contact line cell is supposed to be the cell where the isoline of volume fraction 0.5 lies on. The apparent contact angle is derived from the gradient of volume fraction in this cell.

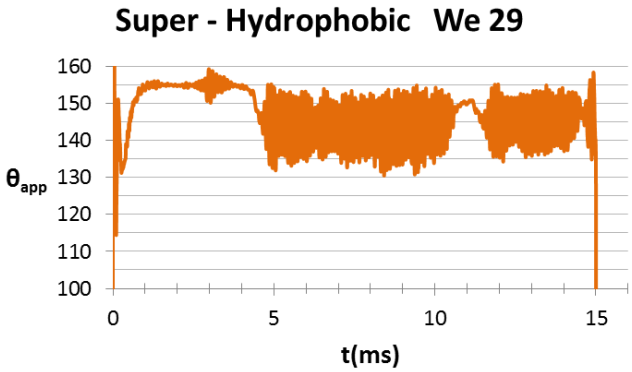

Figure 8. Temporal evolution of the apparent contact angle for Case 3 of Table1.

Conclusions

In this study, a new model for the interaction between a liquid droplet and a solid surface is presented. Based on this model, a force is assumed to act on the contact line as the droplet moves along the surface, but without assuming a constant angle of triple-phase formation, as the conventional one proposed by Brackbill.For hydrophilic surfaces, significant over prediction of maximum radius is observed, for both models, which can be attributed to either the absence of a viscous-friction term in the momentum equation or to the uncertainty which lies on the measurement of the contact angle. For the super-hydrophobic surface, on the other hand, results are much closer to the experimental values, which suggest that as the effect of the solid surface increases (higher contact angle), the contact angle models show a better behavior. For low We number, Marengo's Force Model exhibited almost the same results with those of Brackbill's model, in terms of the temporal evolution of the impingement process. Marengo's Force Model has the significant advantage over all previous methods for the implementation of wettability effects, that the apparent contact angle of the droplet comes as a result of the net force exerted on droplet's rim, rather than inserted as a boundary condition. Therefore, this new model offers a way of observing the impingement phenomenon from a more macroscopic point of view, as the contact angle is

a result of the induced flow and force field. This model needs to be further developed, in order to be more universal and be applicable for a large range of operating conditions. Up to now, results are very promising, so the next step would be to validate the new methodology against measurements of the dynamic contact angle values.

Acknowledgements

The present work was funded by the Marie Curie Fellowship (FP7-PEOPLE-2012-IEF) with Grant Agreement number 329500 funded by the European Commission entitled as "Non Flat Impingement— Droplet Impingement on Non-flat Surfaces". CA acknowledges funding by the Marie Curie Intra-European Fellowship ICE^2 with Grant Agreement 301174.

References

1. Marengo, M., et al., *Drop collisions with simple and complex surfaces.* Current Opinion in Colloid & Interface Science, 2011. **16**(4): p. 292-302.
2. Antonini, C., A. Amirfazli, and M. Marengo, *Drop impact and wettability: From hydrophilic to superhydrophobic surfaces.* Physics of Fluids, 2012. **24**(10): p. 102104-13.
3. Kim, H.Y. and J.H. Chun, *The recoiling of liquid droplets upon collision with solid surfaces.* Physics of Fluids, 2001. **13**(3): p. 643-659.
4. Rioboo, R., M. Marengo, and C. Tropea, *Time evolution of liquid drop impact onto solid, dry surfaces.* Experiments in Fluids, 2002. **33**(1): p. 112-124.
5. Šikalo, Š., et al., *Analysis of impact of droplets on horizontal surfaces.* Experimental Thermal and Fluid Science, 2002. **25**(7): p. 503-510.
6. Sikalo, S., et al., *Dynamic contact angle of spreading droplets: Experiments and simulations.* Physics of Fluids, 2005. **17**(6): p. 062103-13.
7. Hung, Y.-L., et al., *Initial wetting velocity of droplet impact and spreading: Water on glass and parafilm.* Colloids and Surfaces A: Physicochemical and Engineering Aspects, 2011. **384**(1–3): p. 172-179.
8. Vadillo, D.C., et al., *Dynamic contact angle effects onto the maximum drop impact spreading on solid surfaces.* Physics of Fluids, 2009. **21**(12): p. 122002-8.
9. Ashish Saha, A. and S.K. Mitra, *Effect of dynamic contact angle in a volume of fluid (VOF) model for a microfluidic capillary flow.* Journal of Colloid and Interface Science, 2009. **339**(2): p. 461-480.
10. Yokoi, K., et al., *Numerical studies of the influence of the dynamic contact angle on a droplet impacting on a dry surface.* Physics of Fluids, 2009. **21**(7): p. 072102-12.
11. Hirt, C.W. and B.D. Nichols, *Volume of fluid (VOF) method for the dynamics of free boundaries.* Journal of Computational Physics, 1981. **39**(1): p. 201-225.
12. Brackbill, J.U., D.B. Kothe, and C. Zemach, *A continuum method for modeling surface tension.* J. Comput. Phys., 1992. **100**(2): p. 335-354.
13. Theodorakakos, A. and G. Bergeles, *Simulation of sharp gas–liquid interface using VOF method and adaptive grid local refinement around the interface.* International Journal for Numerical Methods in Fluids, 2004. **45**(4): p. 421-439.
14. Nikolopoulos, N., K.S. Nikas, and G. Bergeles, *A numerical investigation of central binary collision of droplets.* Computers & Fluids, 2009. **38**(6): p. 1191-1202.
15. Strotos, G., et al., *Non-dimensionalisation parameters for predicting the cooling effectiveness of droplets impinging on moderate temperature solid surfaces.* International Journal of Thermal Sciences, 2011. **50**(5): p. 698-711.
16. Strotos, G., et al., *Numerical investigation on the evaporation of droplets depositing on heated surfaces at low Weber numbers.* International Journal of Heat and Mass Transfer, 2008. **51**(7–8): p. 1516-1529.
17. Muzaferija, S., et al., *A Two-Fluid Navier-Stokes Solver to Simulate Water Entry.* Proc 22nd Symposium on Naval Hydrodynamics, Washington, DC, 1998: p. 277-289.
18. Olsson, E. and G. Kreiss, *A conservative level set method for two phase flow.* Journal of Computational Physics, 2005. **210**(1): p. 225-246.
19. Sato, Y. and B. Ničeno, *A conservative local interface sharpening scheme for the constrained interpolation profile method.* International Journal for Numerical Methods in Fluids, 2012. **70**(4): p. 441-467.
20. FLUENT 14.5, Theory Guide, 2011.
21. Antonini, C., et al., *General Methodology for Evaluating the Adhesion Force of Drops and Bubbles on Solid Surfaces.* Langmuir, 2009. **25**(11): p. 6143-6154.
22. Pasandideh-Fard, M., et al., *Capillary effects during droplet impact on a solid surface.* Physics of Fluids, 1996. **8**(3): p. 650-659.